Journal of Surface Engineered Materials and Advanced Technology, **2011, 1, 62-72**
doi:10.4236/jsemat.2011.12010 Published Online July 2011 (http://www.SciRP.org/journal/jsemat)

AZ91 Magnesium Alloys: Anodizing of Using Environmental Friendly Electrolytes

N. A. El Mahallawy[1], M. A. Shoeib[2], M. H. Abouelenain[3]

[1]The Design and Production Engineering Department, Faculty of Engineering, Ain Shams University, Cairo, Egypt; [2]Surface Coating Department, Central Metallurgical Research & Development Institute, Helwan, Cairo, Egypt; [3]Petroleum Marine Service, Cairo, Egypt.
Email: nahed.elmahallawy@guc.edu.eg

Received March 14th, 2011; revised May 30th, 2011; accepted June 8th, 2011.

ABSTRACT

An anodizing process, based on environmental friendly electrolyte solutions has been studied on AZ 91 *magnesium alloys by using three types of electrolytes*: *the first is based on sodium silicate, the second on sodium hydroxide-boric acid-borax and the third on sodium silicate-potassium hydroxide-sodium carbonate-sodium tetra borate. A pretreatment including fluoride activation was applied before the anodizing process. It was found that the anodic film thickness increases as current density or anodizing voltage increases. It is also increased with deposition time until the deposition stops due to the formation of a thick anodic film. Optimization of the anodizing conditions - current density and deposition time - was made for each electrolyte. Characterization of anodizing layer was achieved by determination of surface morphology, microstructure, phase analysis, coat thickness, adhesion and corrosion resistance. In all cases, excellent adhesion and corrosion resistance was obtained. A corrosion efficiency ranging from* 94% *to* 97% *was reached*; *the highest value corresponding to the third electrolyte.*

Keywords**:** *Anodizing, Magnesium AZ*91, *Corrosion, Characterization, Environmental Friendly Electrolytes*

1. Introduction

Magnesium and its alloys have received great attention because of their superior properties, such as low density, high specific strength/stiffness, excellent dimensional stability and electromagnetic shielding property, superior damping capacity, high creep strength, good machinability, weldability, high impact resistance, high recyclability, as well as thermal and electrical conductivities [1,2]. They are used in fields where weight reduction is critical or where particular technical requirements are required such as automotive, aeronautic and aerospace including space station, artificial satellite, space shuttle, nuclear energy, electronic and military industries, together with AVCC (Audio video-Computer-Communication) equipment, portable tools, supporting goods, *etc.* [3,4]. However, magnesium and its alloys are highly susceptible to corrosion especially in harsh environmental conditions.

Several techniques have been applied in order to improve the surface properties of magnesium alloys. Anodizing is among the promising techniques for surface protection of Mg alloys; however, most existing anodizing processes use toxic chromate, harmful phosphate or/and fluorides. Therefore, it is still worthy to develop new environmental friendly anodizing processes [5].

In this paper, the anodizing process, based on environmental friendly electrolyte solutions using DC current have been developed to enhance the corrosion resistance of magnesium AZ91alloy. The electrolytes contain none of the chromates, phosphates or fluorides solutions. Optimization of the process parameters was achieved and the anodizing layer was characterized by its adhesion strength, thickness, phase analysis, microstructure, as well as its corrosion resistance on AZ91 magnesium alloys.

2. Experimental Technique

The die-cast Mg alloy AZ91, whose chemical composition is shown in **Table 1**, was prepared as circular discs of 50 mm diameter and 10 mm thickness. The chemical composition was analyzed by Atomic Emission Spectroscopy (AES).

Anodizing experiments were done by using two groups of chemicals: chemicals for pretreatment and chemicals for anodizing processes. The pretreatment procedure used commonly in electroless processes [7], shown in **Table 2**, was applied.

Table 1. Chemical composition of AZ91 Mg alloy (wt%)

Al	Zn	Mn	Si	Cu	Fe	K	Mg
8.77	0.74	0.18	0.01	0.001	0.001	0.01	BAL

Table 2. Pretreatment procedure applied before anodizing process.

Stage no		Name	Symbol	Constituent or condition
1	Mechanical Preparation and Cleaning	Specimens are first polished by using finer grades of waterproof silicon carbide abrasive papers , rinsed in distilled water, supersonic degreasing in acetone and finally dried in air.		
2	Alkaline cleaning	Sodium hydroxide	NaOH	50g/L
		Sodium phosphate	Na_3PO_4	10g/L
			Temperature	Room temperature
			Time	8 - 10 min
	Specimens became brighter than in step one because Mg is passive in alkaline media so that dust, grease… etc were removed from the surface of magnesium alloy.			
3	Acid etching	Chromium trioxide	CrO_3	125 g/L
		Nitric Acid	HNO_3 (70% V/V)	110 ml/L
			Temperature	Room Temperature
			Time	30 - 60 s
	Gross surface scale or oxides are removed and replaced by preferred oxides to be removing later. Etching treatments also provide surface pits to act as sites for mechanical interlocking to improve adhesion.			
4	Fluoride activation	Hydrofluoric acid	HF (40%V/V)	385 ml/L
			Temperature	Room Temperature
			Time	10 min
	Removing residual oxides, that created in the above step and replacing it with a thin layer of MgF_2 .			

Three types of electrolytes were used in anodizing processes. The chemical composition and operating conditions of each type are shown in **Table 3**. The electrolyte cell was built with stainless steel hoop as cathode 10 cm height and 12 cm diameter wide enough to provide an even current distribution. The cell was connected to a DC power supply (MUNK- PSP - VARI-PULS, 10 A, 300 V, USA).The current density and voltage were measured using two digital ammeters (DT 9205 N, China).

In order to optimize the effect of deposition time and current density on the deposition layer thickness, the experiments were divided into two groups: in the first group, the deposition time was varied for the three electrolytes using a constant current density of 20 mA/cm^2; in the second group, the current density was varied while the deposition time was constant. The anodizing process was made at temperature of (30 - 40)˚C .The observation of sparks, which indicates the occurrence of deposition showed that for a time less than 1.5 minutes almost no deposition occurs. The time was increased from 1.5 minutes until the deposition stopped-marked by no sparks. After anodizing processes, the oxide layers obtained were sealed by immersion in boiling distilled water for a time equal to that of the deposition in each case. Sealing of the anodized film is necessary in order to achieve an abrasion and corrosion resistant film by precipitation of hydrated base metal species inside the pores [6,11].

After anodizing, the surface morphology was examined using a scanning electron microscope (SEM) model; JEOL JSM 5410. The grain size of the anodic film was determined by X-ray diffraction (XRD) model; PANalytical X'Pert. The XRD technique, using small-angle X-ray scattering (SAXS) was used to analyze the phases in the anodic coating. The corrosion resistance of anodized coat layer on AZ91D alloy was performed in 3.5 wt% NaCl solution to determine the polarization resistance at ambient temperature using AUTOLAB PGSTAT 30

The anodic film thickness was measured by the coating thickness meter (posi-tector 6000 FN). Hydraulic adhesion tester (Elcometer 108) measured the adhesion of the anodic film. The microhardness measurements

Table 3. Chemical composition and operating conditions of electrolytes.

Electrolyte (1) [8]	
sodium silicate (Na_2SiO_2)	122 g/l
Temp	(30 - 40)˚C
Current density	16 mA/cm^2 to 31 mA/cm^2
Deposition time (minute)	1.5 to 11
Electrolyte (2)[9]	
Sodium hydroxide (NaOH)	50.0 g/L
Boric acid(H_3BO_3)	10.0 g/L
Borax or hydrous sodium borate ($Na_2B_4O_7.10H_2O$)	20.0 g/L
Temp	(30 - 40)˚C
Current density	16 mA/cm^2 to 20 mA/cm^2
Deposition time (minute)	1.5 to 9
Electrolyte (3)[10]	
Sodium silicate (Na_2SiO_3)	50 g/l
Potassium hydroxide (KOH)	50 g/l
Sodium carbonate (Na_2CO_3)	50g/l
Sodium tetra borate (Borax $Na_2B_4O_7$)	30 g/l
Temp	(30 - 40)˚C
Current density	16 mA/cm^2 to 31 mA/cm^2
Deposition time (minute)	1.5 to 9

were carried out by the hardness tester model Shimdsu type M, and the surface roughness by Elcometer 223. The microhardness measurements of coat layers were performed on specimens cross-sections using 50-gram load for 15 seconds.

3. Results and Discussion

3.1. Effect of Pretreatment on Surface Morphology

Study of the surface morphology after the pretreatment procedure, shown **Figure 1**, indicates the formation of pits, which is expected to improve the adherence of coat layer to the substrate. The use of fluoride activation in the pretreatment is also expected to add a layer of MgF_2 which minimizes the effect of local corrosion cells by creating an equipotentialized surface [7].

3.2. Effect of the Deposition Time on the Coating Thickness

Figure 2 shows that the coat thickness for the three electrolytes increases with the deposition time, rapidly in the first 3 minutes then with a slow rate after 3 to 9 minutes until it levels off after 9 minutes. This behavior is due to the increase in the thickness of the coat layer acting as a barrier to the flow of current, which decreases the rate of oxidation of magnesium. From the results, the optimum deposition time used to obtain maximum coat thickness was 9 minutes for the three electrolytes at the same operating conditions with 20 mA/cm^2 current density. In general, the coat thickness was the highest for electrolyte (1) - 42 µm, followed by electrolyte (2) - 32 µm, then electrolyte (3)-28 µm.

Comparison between the maximum coating thickness obtained in the present work and previous work [8-10] indicates a general agreement, however, difference in values are obtained due to the difference in base metal composition, current density and temperature. For example, for electrolyte 1, maximum coating layer thickness was 42 µm while in previous work [8] on AZ91, the anodic film was 25 µm at 60 C, 20mA/Cm2 and 9 minutes coating time. The large thickness in the present work is due to the lower anodizing temperature. This explanation is based on previous work [12,13], which

i n d i c a t e s t h a t

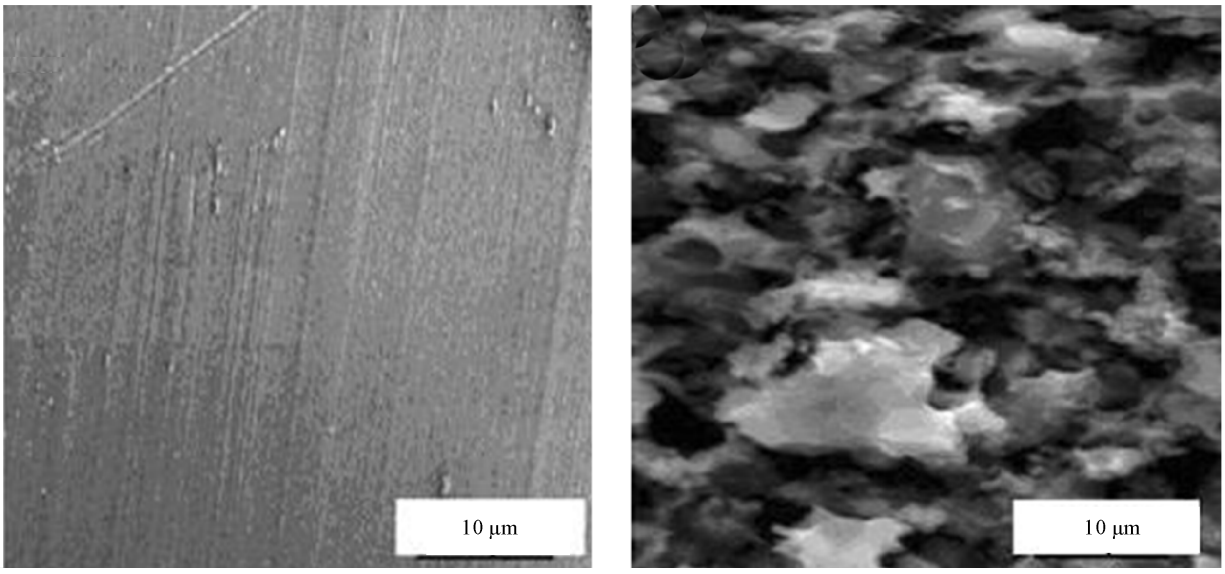

Figure 1. Surface morphology of the AZ91 magnesium alloy (a) before pre-treatment (b) after pre-treatment.

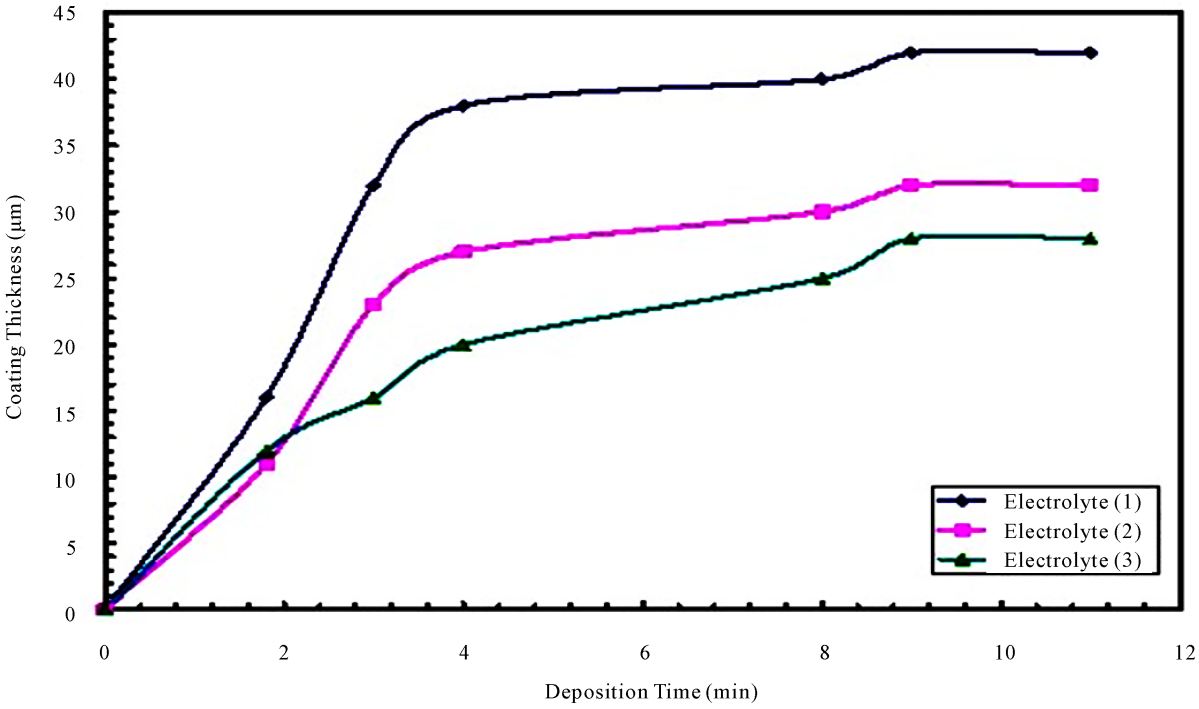

Figure 2. Effect of deposition time on coat thickness by using three electrolytes and pre-treatment procedure at temp. (30 - 40)˚C and constant current density –DC-20 mA/cm^2.

the temperature and coat thickness are inversely proportional.

3.3. Effect of Current Density on Coating Thickness

The current density is a main electric parameter in anodizing. **Figure 3** shows the effect of current density on coat thickness for the three types of electrolytes, using a deposition time of 9 minutes (optimum) at a temperature (30 - 40)˚C. With increasing current density, the driving

force for anodizing increases, which enhances the coat development and formation. The thickness increased first

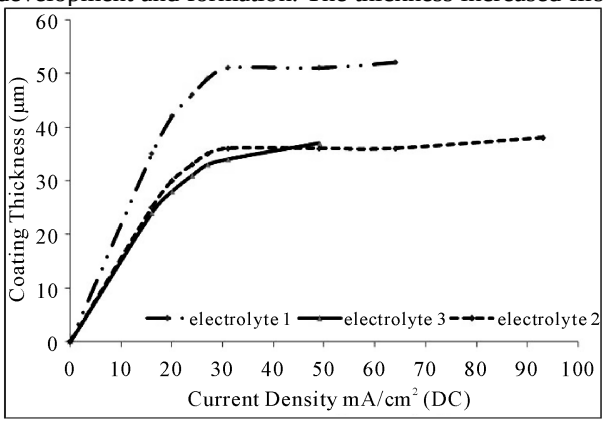

Figure 3. Effect of current density on coating thickness by using three electrolytes and constant deposition time at 9 minutes.

rapidly up to 20 mA/cm^2 then the rate slowed down until almost no increase in thickness of the deposited oxide layer was obtained. This threshold current density was 25mA/cm^2 for electrolyte (1) and (3) and 20 mA/cm^2 for electrolyte (2), resulting in coat thickness of 50 µm for electrolyte (1) and 30 µm for electrolytes (2) and(3).

For coat development, there are three ways by which anions move to the anode, mainly diffusion, convection and electric migration [14]. The latter being the main one during anodizing. It can be said that as the anodizing layer thickness increases beyond a certain value, the electric migration is suppressed due to the higher resistivity of the formed oxide layer marked by stop of sparking.

3.4. Oxide Formation Mechanism

The anodizing process is a dynamic equilibrium of partial processes of oxide formation, the others. The mechanism of anodizing process could be explained dissolution, and oxygen evolution. The dominance of one partial process will suppress according to the growth of anodic film, in which the pre-existing film was strengthened, modified or substituted repeatedly by sparking/break- down events. The sparking occurs by the action of the strong electric field created during anodization. Anions in the electrolyte first need to arrive at the anode/elec- trolyte interface and then enter into anodic coatings [15].

The general reactions, occurring in the anodizing process for Mg, are as follow:

$$Mg \rightarrow Mg^{2+} + 2e^- \quad (1)$$

$$4OH^- \rightarrow O_2 \uparrow + 2H_2O + 4e^- \quad (2)$$

$$Mg^{2+} + 2OH^- \rightarrow Mg(OH)_2 \quad (3)$$

$$Mg(OH)_2 \rightarrow MgO + H_2O \quad (4)$$

$$Mg(OH)_2 + SiO_2 \rightarrow Mg_2SiO_4 \quad (5)$$

During the oxidation process, the Mg ions, produced by reaction (1), combine with the OH^- in the electrolyte solution to form $Mg(OH)_2$ and Mg_2SiO_4 (reactions (3) and (5), respectively). Due to the thermal energy from the sparks in the PEO process, the hydroxides change to oxide compounds by the dehydration process, reaction (4). The coating formation processes, reactions (3), (4) and (5) may be promoted by a high concentration of the electrolyte, containing more SiO_2 and OH^- ions.

Based on previous observations during anodizing of AZ 91 magnesium alloy [5], formation and dissolution of oxide/hydroxide films occur simultaneously. The present results indicate that the anodic film growth is dominant up to 20 - 25 mA/cm^2, beyond which the thickness of the oxide layer remains almost constant due to the break-down and/or dissolution of this thin film as previously noticed.

3.5. Surface Morphology of Anodic Coat

The surface morphology of anodic coat, **Figures 4-6**, revealed the presence of pores with different shapes and sizes distributed all over the surface. However, the pores are very small and do not have full penetration to the substrate surface. Different pore size and density were observed depending on the electrolyte. Electrolyte (1) created many pores of approximately 7 µm diameter, **Figure 4**, while electrolyte (2) created a few pores of approximately 1 µm diameter, **Figure 5**, and electrolyte (3) created a few pores of (2 - 3) µm diameter, **Figure 6**. These differences in pore diameters result from the differences of spark behavior and evolution of gases, as in electrolyte (1) the spark was stronger and accompanied with higher evolution of gases compared to electrolytes (2) and (3).

Micro cracks are also visible on the coat surface. They are formed due to thermal stresses resulting from rapid cooling of the oxides by the electrolyte acting as a coolant.

Difference crack sizes are also observed in the coat layer due to the presence of different oxides, with different shrinkage rates [16,17] depending on the type of electrolyte (see next paragraph), **Figures 4-6**.

The cracks are probably formed in week regions, where the localized film layers were destroyed prior to other regions. However, new anodizing products formed in/around the broken regions rapidly and intensively so that the existing microdefects were filled up or mended by the fresh products. This is clear from the occurrence of cracks on the surface but not reaching the depth.

3.6. Phase Analysis in Coat Layer Using XRD and EDX

X-ray diffraction patterns of the specimen anodized by

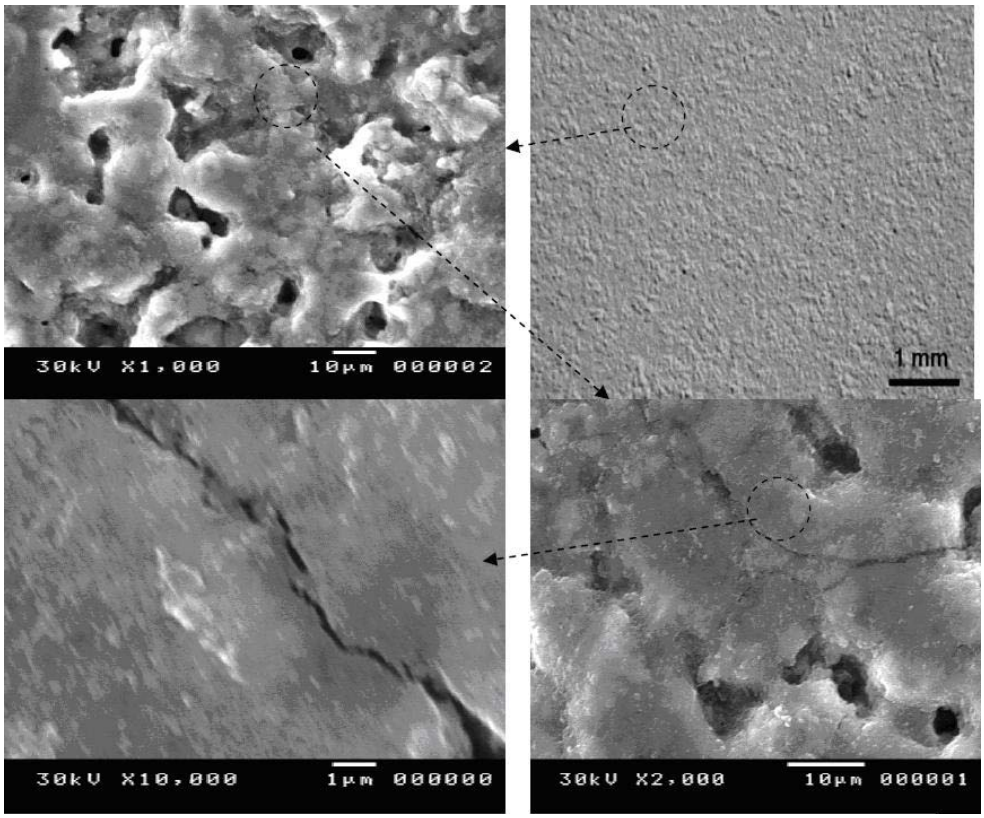

Figure 4. SEM morphology showing the coat surface using electrolyte (1).

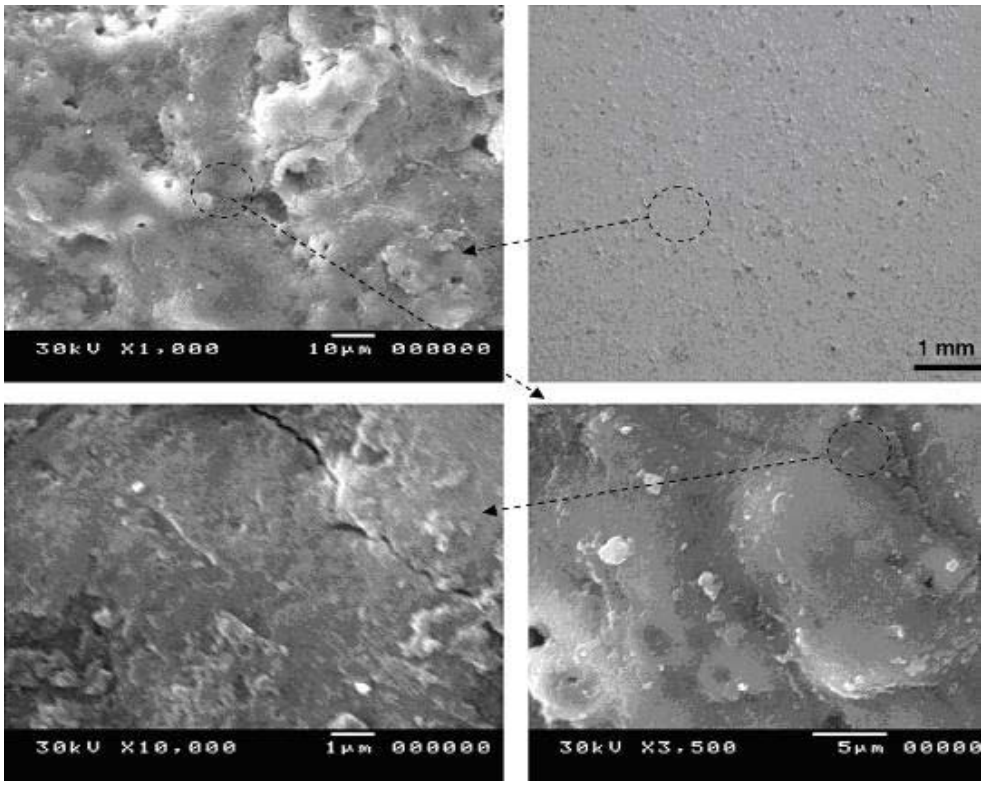

Figure 5. SEM morphology showing the coat thickness using electrolyte (2).

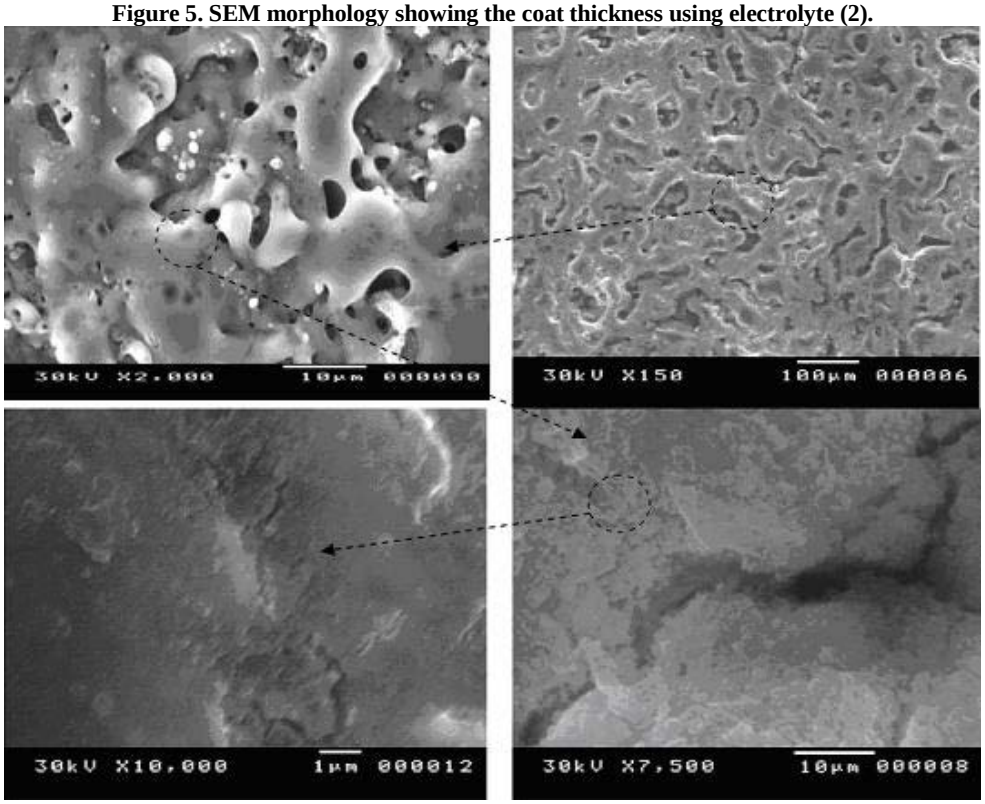

Figure 6. SEM morphology showing the coat surface using electrolyte (3).

using electrolyte (1), **Figure 7**, indicate that the dominating phase is MgO, followed by smaller amounts of SiO_2 and Mg as shown in **Table 4**, while in case of electrolyte(2), the dominating phase is MgO, Mg and B_2O_3. For electrolyte (3), the dominating phase is MgO, followed by SiO^2, Mg and Mg_2SiO_4. The occurrences of these phases indicate that the substrate and the electrolyte both contribute in forming the coat layer.

The EDX analysis across the anodic coat layer, **Table 5**, indicates that the percentage of oxygen and silicon decreases from the surface towards the substrate (zone III > zone II > zone I). This indicates that the coat layer acts as a barrier to decrease the rate of oxidation of magnesium. It was found previously [18] that when a relatively thick coating was established, an excessive oxygen evolution is observed. This could explain the increase in oxygen at the expense of the Mg on the outer layer.

3.7. Microstructure of the Coat Layers and Crystal Size

The cross-section view of the coat layers for all three electrolytes, **Figure 8**, shows that anodized coating films are relatively uniform in thickness and that the pores are present but do not completely extend to the base metal. Pores result from the generation of sparks and evolution of gases from the hydrolysis of water [16]. These pores are relatively uniform in distribution.

The crystal size of the anodic coat determined by X-ray diffraction (XRD), indicate that all crystal phases are in the nano scale with sizes 4 to 5 nm, **Table 6**. This means that the three electrolytes result in almost similar crystal size, as the MgO is the dominating phase in all coats.

3.8. Coat Adhesion

An excellent adhesion exceeding 18 MPa between the anodic film and the substrate was found for all specimens. This value is larger than for electroless nickel plating on anodized magnesium alloy (about 11 MPa) [19]. This adhesion is enhanced by the formation of pits formed by the pretreatment procedure, which increased the surface roughness and contributed to increased adhesion of the coat layer as reported by Adachi *et al.* [20]. In additions, the analysis of the obtained anodic film layers showed that they contain (Mg - MgO- Mg_2SiO_4). This indicates that the metallic substrate has diffused into coating layer, resulting in further enhancement of the adhesion.

3.9. Surface Roughness

Ten surface roughness measurements were taken on the surface of the specimens and the results in **Figure 9** indicate that the surface roughness ranges from 13 µm to

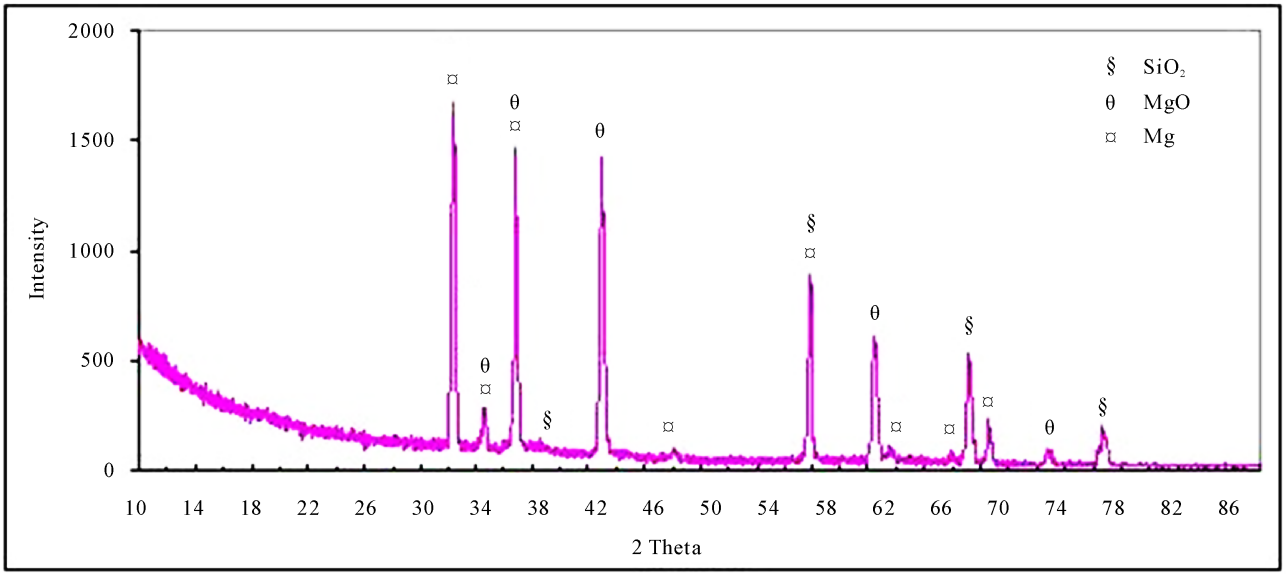

Figure 7. XRD spectra of the anodic coatings by using electrolyte (1), [temp. (30 - 40)°C, deposition time 9 min and current density 31 mA/cm^2].

Table 4 Phases present in coating layer using the different electrolytes.

Compound name	Chemical formula	Score	Percentage (wt%)
Electrolyte (1)			

Magnesium	Mg	31	0.25
Periclase	MgO	68	0.55
Silicon Oxide	SiO_2	25	0.20
	Electrolyte (2)		
Magnesium	Mg	53	0.3
Periclase	MgO	75	0.42
Ceramic Oxide Or (Boric oxide)	B_2O_3	51	0.28
	Electrolyte (3)		
Magnesium	Mg	52	0.28
Silicon Oxide	SiO_2	47	0.25
Periclase	MgO	69	0.37
Forsterite	Mg_2SiO_4	16	0.10

Table 5. EDX analysis of anodic coat layer (wt%).

Zone No.	O%	Mg%	Al%	Si%
Zone I (close to the Mg)	27.7	33.4	0.9	37.8
Zone II (central region)	29.2	27.6	0.8	42.2
Zone III (close to surface)	31.1	24.3	0.7	43.7

*The EDX analysis of the anodic coat layer by using electrolyte (3) after the pretreatment, deposition time 9 min and current density 31 mA/cm^2 at temp. (30 - 40)˚C.

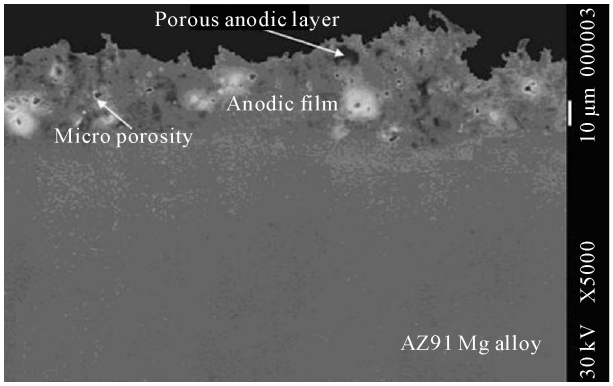

(a)

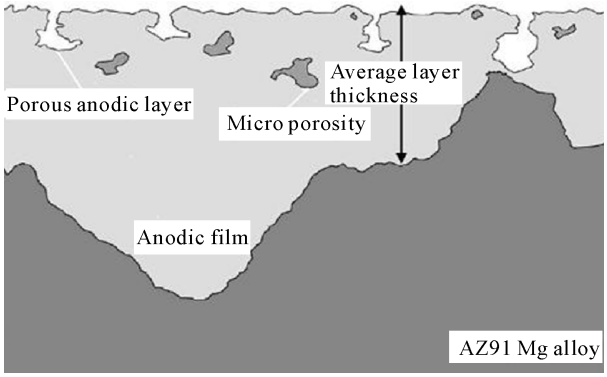

(b)

Figure 8. (a) Cross section morphology (b) sketch of a typical cross section, for anodic coating of anodic coating film on magnesium alloy AZ91D at 31 mA/cm^2 current density, 9 minutes deposition time and temperature (30 - 40)˚C.

Table 6. Crystalline size for the coat layers for the three electrolytes.

Type of bath	Crystal size (nm)
Electrolyte (1)	5.1
Electrolyte (2)	3.95
Electrolyte (3)	4.12

24 µm. It increases by increasing the current density and is lower for electrolyte (2). In addition, **Figure 10** shows that the surface roughness increases by increasing the coating thickness. For electrolyte (2), the surface roughness was found to be constant for current density ranging from 24 mA/cm^2 to 31 mA/cm^2, which corresponds to an almost constant coat thickness, as indicated in **Figure 3**.

The surface roughness is partly related to the non-homogeneity of coat layer and the formation of pores and cracks on the anodic film layers. These surface defects

were greater in case of electrolyte (1) followed by (3) and (2).

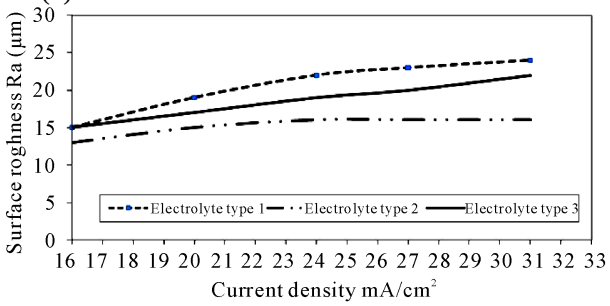

Figure 9. Effect of change of current density on surface roughness of coating layers by using three electrolytes at temperature (30 - 40)˚C and constant time 9 minutes.

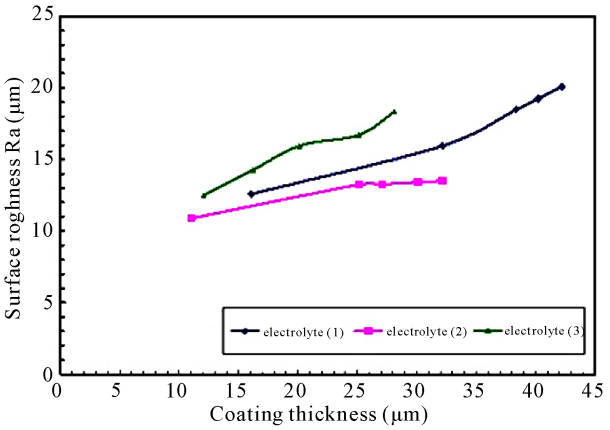

Figure 10. Relation between coating thickness and surface roughness for anodizing process by using three electrolytes, pre-treatment procedure 9 minute deposition time, and current density (16 to 31) Am/cm^2.

3.10. Microhardness

The results indicate that the microhardness increases with increasing the current density, **Figure 11**, and coat thickness, **Figure 12** reaching value of 570 VHN for electrolyte (3) with 28 µm thickness. This is expected as the coat phases include MgO and SiO_2 hard phases. **Table 5** indicates that the Si increases towards the coat surface which could results in higher concentration of the SiO_2 hard phase. In general, the hardness of the coat phases is higher than that of the magnesium substrate (VHN = 360 HV).

3.11. Corrosion Tests

Figure 13 shows potentiodynamic curves obtained for AZ91 magnesium alloys before and after anodizing processes by using the three electrolytes. Potentiodynamic curves for the anodized specimens are shifted in the noble direction indicating a higher corrosion resistance.

The electrolytes can be ranked to give the best anti-corrosion properties as electrolyte (3) followed by (2),

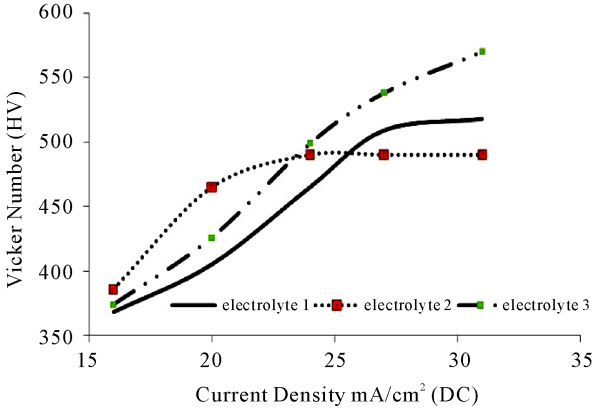

Figure 11. Effect of change current density in microhardness of coating layers by using three electrolytes at temperature (30 - 40)˚C and time at 9 minute.

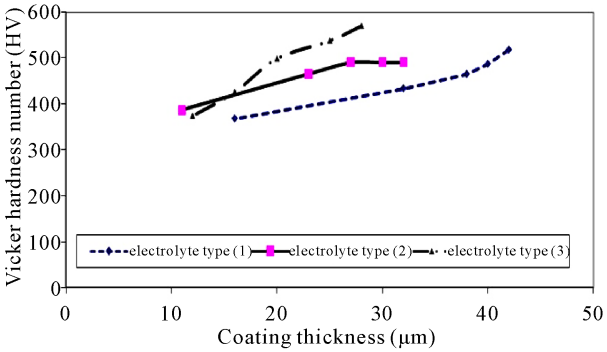

Figure 12. Relation between coating thickness and microhardness of coating layers for anodizing process by using three electrolytes.

then by (1). The results of linear polarization experiments summarized in **Table 7** shows that the corrosion resistance of AZ91 magnesium alloys is enhanced significantly by using the three electrolytes in anodizing processes. This is marked by the increase of R_p, decrease in Icorr and shift of E_{corr} in the noble direction (more positive values). The corrosion rate drops from 57.48 mpy to 3.39, 2.64 and 1.70 mpy using electrolytes (1), (2) and (3) reaching excellent efficiency of 94%, 95% and 97% respectively.

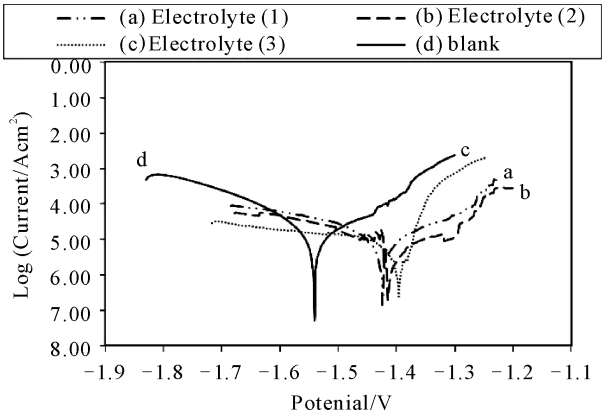

Figure 13. Potentiodynamic polarization curves for the anodized specimens by using three-electrolyte to gather with the AZ91 Mg Substrate (Blank).

4. Conclusions

1) The anodizing process of AZ91 based on environmental friendly electrolytes was successful to form a smooth anodic film, with high corrosion resistance and excellent bonding strength to substrate. The solutions used were sodium silicate for electrolyte (1), sodium hydroxide - boric acid - borax for electrolyte (2), sodium silicate-potassium hydroxide- odium carbonate-sodium tetra borate for electrolyte (3),

2) The anodized layer included the MgO phase as the dominating phase followed by smaller amounts of SiO_2, MgO, B_2O_3 and Mg_2SiO_4 indicating that the substrate and the electrolyte both contribute in forming the coat layer.

3) High improvement in corrosion is due to the formation of anodic film with layer thickness between 30 micron (electrolyte (2) and (3)) and 50 micron (electrolyte (1)) with excellent adhesion to the magnesium substrate. The higher improvement in corrosion resistance is associated with less microcracks and micropores in the coat which in all cases do not reach the Mg substrate.

4) The best anticorrosion performance was obtained for electrolyte (3) where the corrosion resistance efficiency 97% was reached, while it was 94% and 95% for electrolyte (1) and (2) respectively.

Table 7. Results of linear polarization experiments.

Specimen for	E_{corr}, V	R_p, $\Omega.cm^2$	I_{corr}, $\mu A/cm^2$	Corrosion Rate, mpy	Efficiency
AZ91 Mg substrate (Blank)	–1.585	4.168 E+2	5.027×10^{-5}	57.481	----------
Electrolyte (1)	–1.427	1.863E+3	4.171E-6	3.39	94.10%
Electrolyte (2)	–1.394	2.71E+3	3.193 E-6	2.64	95.40%
Electrolyte (3)	–1.371	3.67E+2	2.093 E-6	1.70	97.04%

*Efficiency = **(** Corrosion Rate for Mg blank - Corrosion Rate using Electrolyte **)**/Corrosion Rate for Mg blank.

REFERENCES

[1] G. L. Song, A. Atrens, D. Stjohn, J. Nairn and Y. Li, "The Electrochemical Corrosion of Pure Magnesium in 1N NaCl," *Corrossion Science*, Vol. 39, No. 5, 1997, pp.855-856. doi:10.1016/S0010-938X(96)00172-2

[2] A. J. Zozulin and D. E. Bartak, "Anodized Coatings for Magnesium Alloys," *Metal Finishing*, Vol. 92 No. 3, 1994, pp.39-42.

[3] J. E. Gray and B. Luan, "Protective Coatings on Magnesium and Its Alloys — A Critical Review," *Journal of Alloys Compounds*, Vol. 336, No. 1-2, 2002, pp. 88-13. doi:10.1016/S0925-8388(01)01899-0

[4] E. Ghali and W. Dietzel, "General and Localized Corrosion of Magnesium Alloys: A Critical Review," *Journal of Materials Engnerring and Performance*, Vol. 13, No. 1, 2004, pp. 7-23. doi:10.1361/10599490417533

[5] Y. Zhang, C. Yan, F. Wang, H. Lou and C. Cao, "Study on the. Environmentally Friendly Anodizing of AZ91D Magnesium Alloy," *Surface and Coating Technology*, Vol. 161, No. 1, 2002, pp. 36-43. doi:10.1016/S0257-8972(02)00342-0

[6] C. K. Mittal, "Chemical Conversion and Anodized Coatings," *Transactions of the Metal Finishers Association of India*, Vol. 4, 1995, pp. 227-231.

[7] A. K. Ehmeda "Anodizing of Magnesium Alloy (AZ91D) in Extreme Alkaline and Acidic Media," MSC Thesis, Tabbin Institute for Metallurgical Studies, Cairo, 2008

[8] W. Li , L. Zhu and H. Liu , "Preparation of Hydrophobic Anodic Film on AZ91D Magnesium Alloy in Silicate Solution Containing Silica Sol," *Surface and Coatings Technology*, Vol. 201, No. 6, 2006, pp. 2573-2577. doi:10.1016/j.surfcoat.2006.04.068

[9] C. S. Wu, Z. Zhang, F. H. Cao, L. J. Zhang, J. Q. Zhang and C. N. Cao, "Study on the Anodizing of AZ31 Magnesium Alloys in Alkaline Borate Solutions," *Applied Surface Science*, Vol. 253, No. 8, 2007, pp. 3893-3898. doi:10.1016/j.apsusc.2006.08.020

[10] M. Hara, K. Jimatsuda, W. Yamauchi, M. Sakaguchi and T. Yoshikata. "Optimization of Environmentally Friendly

Anodic Oxide Film for Magnesium Alloys," *Materials Transactions*, Vol. 47, No. 4, 2006, pp. 1013-1019. doi:10.2320/matertrans.47.1013

[11] O. Khaselev, J. Yahalom and J. Electrochem. "Constant Voltage Anodizing of Mg-Al Alloys in KOH-Al (OH) (3) Solutions," *Journal of the Electrochemical Society*, Vol. 145, No. 1, 1998, pp. 190-193. doi:10.1149/1.1838234

[12] A. K. Sharma, R. Uma Rani and K. Giri, "Studies on Anodization of Magnesium Alloy for Thermal Control Applications," *Metal Finishing*, Vol. 95, No. 3, 1997, pp.43-54. doi:10.1016/S0026-0576(97)86772-4

[13] J. Yahalom and J. Zahavi, "Experimental Evaluation of Some Electrolytic Breakdown Hypotheses," *Electrochimica Acta*, Vol. 16, No. 5, 1971, pp. 603. doi:10.1016/0013-4686(71)85169-1

[14] R. F. Zhang, D. Y. Shan, R. S. Chen and E. H. Han, "Effects of Electric Parameters on Properties of Anodic Coatings Formed on Magnesium Alloys," *Materials Chemistry and Physics*, Vol. 107, No. 2-3, 2008, pp. 356-363. doi:10.1016/j.matchemphys.2007.07.027

[15] Y. Zhang and C. Yan, "Development of Anodic Film on Mg Alloy AZ91D," *Surface and Coatings Technology*, Vol. 201, No. 6, 2006, pp. 2381-2386. doi:10.1016/j.surfcoat.2006.04.015

[16] X. Zhou, G. E. Thompson, P. Skeldon, G. C. Wood, K. Shimizu and H. Habazaki, "Film Formation and Detachment During Anodizing of Al-Mg Alloys", *Corrosion Science*, Vol. 41, No. 8, 1999, pp. 1599-1605. doi:10.1016/S0010-938X(99)00007-4

[17] H. F. Guo, M. Z. An, H. B. Huo and S. Xu, "Microstructure Characteristic of Ceramic Coatings Fabricated on Magnesium Alloys by Micro-Arc Oxidation in Alkaline Silicate Solutions," *Applied Surface Science*, Vol. 252, No. 22, 2005, pp. 2187-2191. doi:10.1016/j.apsusc.2005.09.067

[18] P. Zhang, X. Nie and D. O. Northwood, "Influence of Coating Thickness on the Galvanic Corrosion Properties of Mg Oxide in an Engine Coolant," *Surface and Coating Technology*, Vol. 203, No. 20-21, 2009, pp. 3271-3277. doi:10.1016/j.surfcoat.2009.04.012

[19] S. Sun, J. Liu, C. Yan and F. Wang, "A Novel Process for Electroless Nickel Plating on Anodized Magnesium Alloy," *Applied Surface Science*, Vol. 254, No. 16, 2008, pp. 5016-5022. doi:10.1016/j.apsusc.2008.01.169

[20] S. Adachi and K.Nakata, "A Novel Process for Electroless Nickel Plating on Anodized Magnesium Alloy," *Plasma Processes and Polymers*, Vol. 4, No. S1, 2007, pp. 512-515. doi:10.1002/ppap.200731217

